J Mater Sci (2006) 41:6138–6141
DOI 10.1007/s10853-006-0423-y

LETTER

Effects of precursors in the ethanol-based sol–gel synthesis of Zn_2SiO_4:Mn phosphor

C. J. Kim · M. S. Kwon

Received: 7 March 2006 / Accepted: 8 May 2006 / Published online: 12 August 2006

Zn_2SiO_4:Mn is an efficient green-light-emitting phosphor for lamps, plasma display panels (PDP), electroluminescene (EL) devices, and liquid crystal display (LCD) backlights due to its high photoluminescent efficiency and chemical stability [1–5].

The authors reported simple sol–gel synthesis and green luminescence of nanocrystalline Zn_2SiO_4:Mn phosphor instead of the traditional high-temperature, solid-state reaction with a micron-sized phosphor [6]. The sol–gel process is a very flexible low-temperature process for synthesizing nanosized materials [7]. It allows one to easily obtain the desired composition as well as a high degree of uniformity. In the authors' previous study, only zinc acetate and manganese chloride were used as zinc and manganese precursors, respectively [6].

The results of an ongoing study of the effects of the zinc and manganese precursors for the sol–gel route are reported herein. Ethanol was used as a solvent, as in the authors' previous study. Moreover, all the processes were performed in a simple air environment, requiring no further reducing heat treatment. Two kinds of zinc precursors were used, namely: zinc acetate dehydrate [$Zn(CH_3COO)_2 \cdot 2H_2O$] and zinc nitrate [$Zn(NO3)_2 \cdot 6H_2O$]. Manganese precursor was also selected over manganese chloride ($MnCl_2 \cdot 4H_2O$), manganese sulfate ($MnSO_4 \cdot 4H_2O$), and manganese acetate ($Mn(CH_3COO)_2 \cdot 4H_2O$).

The initial manganese composition was set to produce the final composition of $Zn_{2-x}Mn_xSiO_4$ ($x = 0.04$) phosphors for each combination of precursors. A fixed molar amount of zinc precursor and tetraethoxysilane (TEOS) was dissolved in ethanol and then stirred for 30 min at room temperature. The manganese precursor was then added to the solution, after which the solution was stirred for another 30 min. Finally, NH_4OH was added to the solution to change its initial pH to 11, as in the authors' previous study [6]. The final solution was dried in the air at 120 °C for 15 h, after which it was transformed into dried amorphous gel powders. The gel powder that was obtained was finally fired at 1000 °C in air for 1 h to induce the crystallization of the dried gel powder. X-ray diffraction (XRD) was used to identify the crystalline phases of the sol–gel-synthesized Zn_2SiO_4:Mn phosphors. FE-SEM was used to obtain the phosphor powder images. The photoluminescence was measured using a Hitachi F-4500 fluorescence spectrometer with a 150 W monochromatized Xe lamp, using an excitation wavelength of 254 nm and a 430 nm cut-off to eliminate harmonic or scattering peaks.

Figure 1 shows the XRD patterns of the sol–gel-derived $Zn_{2-x}Mn_xSiO_4$ ($x = 0.04$) phosphors prepared from the different combinations of the zinc and manganese precursors. Figure 1 shows the strong dependency of the formation of single-crystalline-phase Zn_2SiO_4 on the use of zinc and manganese precursors. A strong evidence of the residual ZnO phase can also be seen in zinc acetate with manganese sulfate, zinc acetate with manganese acetate, zinc nitrate with manganese chloride, and zinc nitrate with manganese sulfate. The residual peaks agree well with the standard pattern of the ZnO of JCPDS Card No. 36-1451 (space

C. J. Kim · M. S. Kwon (✉)
Department of Materials Science and Engineering,
University of Seoul, 90 Jeonnong-dong, Dongdaemun-gu,
Seoul 130-743, South Korea
e-mail: mskwon@uos.ac.kr

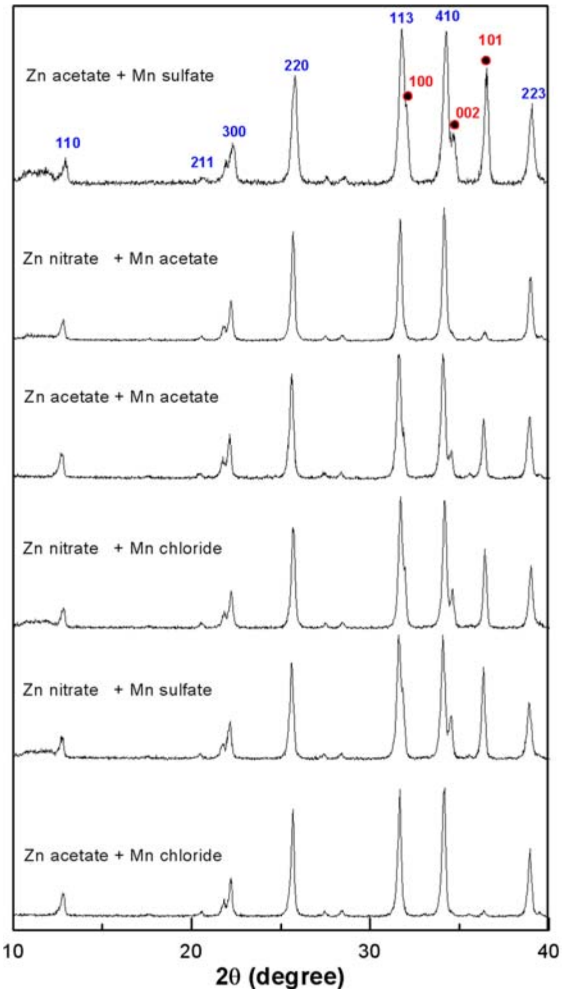

Fig. 1 XRD patterns of the sol–gel-derived $Zn_{2-x}Mn_xSiO_4$ ($x = 0.04$) phosphors with different combinations of precursors

group number 186). Zinc nitrate with manganese acetate, and zinc acetate with manganese chloride, however, show the suppression of the ZnO residual phase and an almost complete formation of the single phase of crystalline Zn_2SiO_4 only, as can be seen in Fig. 1. Their diffraction peaks can be assigned to Willemite (JCPDS Card No. 37-1485, space group number 148). The zinc acetate and manganese chloride combination produced the same result as in the authors' previous study. Therefore, the use of the zinc and manganese precursors combination is critical to obtaining the single phase of the Zn_2SiO_4 host in the authors' ethanol-based sol–gel route.

Figure 2 shows the FE-SEM images of the sol–gel-derived $Zn_{2-x}Mn_xSiO_4$ ($x = 0.04$) phosphors fired at 1000 °C with different precursor combinations. Figure 2 and the calculated crystallite size showed the nanosized $Zn_{2-x}Mn_xSiO_4$ ($x = 0.04$) phosphors to be less than 200 nm on average.

Figure 3 shows the green emission spectra of the sol–gel-derived $Zn_{2-x}Mn_xSiO_4$ ($x = 0.04$) phosphors excited by 254 nm UV for the different precursor combinations. The green emission band in Fig. 3 agrees well with the literature value that was assignedto an electronic transition of $^4T_1(^4G) \rightarrow {}^6A_1(^6S)$ peaking around the wavelength 525 nm, and which is a parity-forbidden emission transition of Mn^{2+} ions [3, 8]. Figure 3 shows that the two strongest emission bands are the combinations of zinc nitrate and manganese acetate, and of zinc acetate and manganese chloride. These combinations showed the suppression of the ZnO residual phase and showed the formation of single phase of the Zn_2SiO_4 host, as can be in Fig. 1.

Figure 4 shows the excitation spectra of the same $Zn_{2-x}Mn_xSiO_4$ ($x = 0.04$) phosphors, focusing on the 524 nm emission, as can be seen in Fig. 3. Each excitation spectrum shows an excitation band that mainly corresponds to the charge transfer transition (or the ionization of manganese) from the divalent manganese ground state (Mn^{2+}) to the conduction band (CB) [8]. The tendency of the relative excitation intensity is similar to that of the emission intensity, as can be seen in Fig. 3. Thus, the most efficient excitation from the charge transfer mechanism and the suppression of residual ZnO formation seem to lead to the maximum emission intensity.

Figure 5 shows the photoluminescence decay curves of the sol–gel-synthesized $Zn_{2-x}Mn_xSiO_4$ ($x = 0.04$) phosphors with different combinations of precursors. The decay curves represent phosphorescene life times. The decay time τ was simply measured at the position where the intensity decreased by $1/e$ of the initial intensity. The decay time for zinc acetate with manganese chloride was shown to be 34 ms, while it was shown to be 33 ms for the same precursor combination in the authors' previous study [6]. The combination of zinc nitrate and manganese acetate, however, was shown to have a decay time of 43 min, and showed the strongest emission, as can be seen in Fig. 3. Therefore, to apply the sol–gel-derived $Zn_{2-x}Mn_xSiO_4$ ($x = 0.04$) phosphors to a PDP pixel, a careful engineering trade-off between emission intensity and decay time is needed for each combination of precursors.

The effects of the precursor selections on the ethanol-based sol–gel synthesis of the $Zn_{2-x}Mn_xSiO_4$ phosphors, particularly for the single-phase formation of the host oxide, emission intensity, excitation efficiency, and decay time, were shown herein.

Fig. 2 FE-SEM images of the sol–gel-derived $Zn_{2-x}Mn_xSiO_4$ (x = 0.04) phosphors with different combinations of precursors

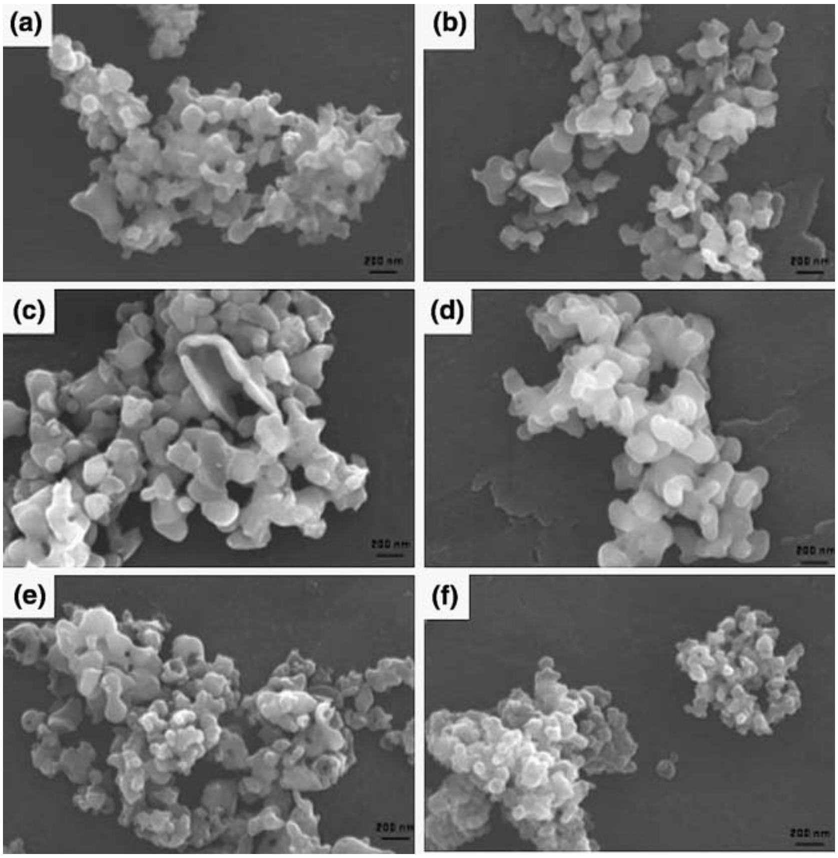

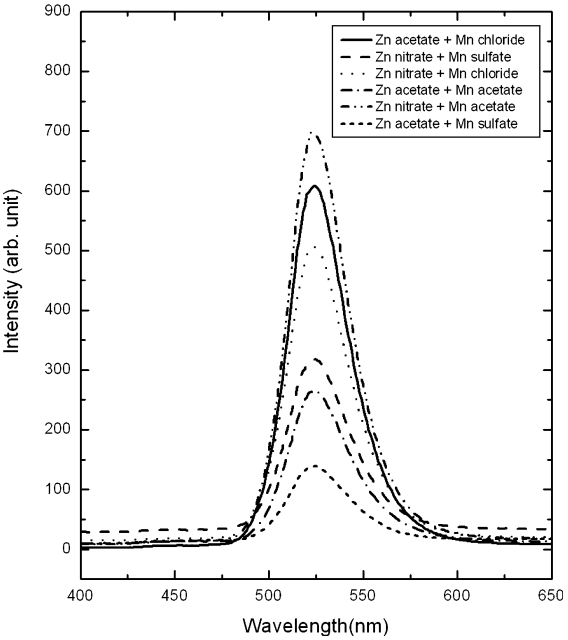

Fig. 3 Emission spectra excited by 254 nm of the sol–gel-derived $Zn_{2-x}Mn_xSiO_4$ (x = 0.04) phosphors with different combinations of precursors

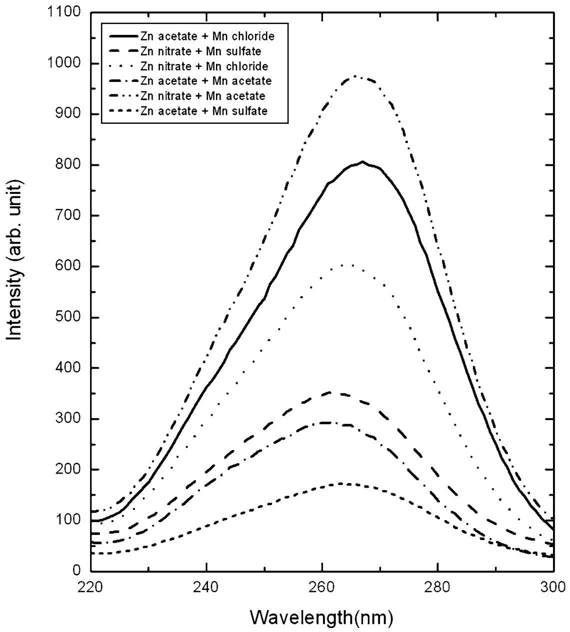

Fig. 4 Excitation spectra of the sol–gel-derived $Zn_{2-x}Mn_xSiO_4$ (x = 0.04) phosphors with different combinations of precursors (the emission wavelength that was monitored was 524 nm)

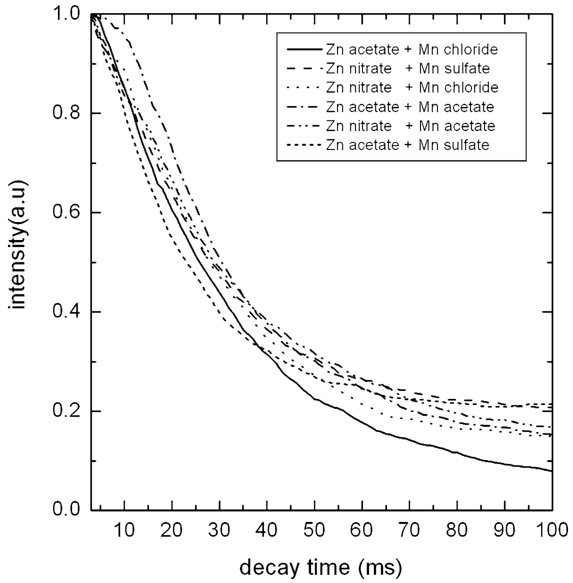

Fig. 5 Photoluminescene decay curves of the sol–gel-derived $Zn_{2-x}Mn_xSiO_4$ ($x = 0.04$) phosphors with different combinations of precursors

References

1. Shionoya S, Yen WM (1999) In: Phosphor handbook, vol 2. CRC Press, Boston, p 629
2. Copeland TS, Lee BI, Qi J, Elrod AK (2002) J Luminescence 97:168
3. Bhatkar VB, Omanwar SK, Moharil SV (2002) Phys Stat Sol A 191:272
4. Zhang QY, Pita K, Kam CH (2003) J PhysChem Mater 64:333
5. Lin J, Sanger DU, Mennig M, Barner K (1999) Mat Sci Eng B 64:73
6. Kwon MS, Kim CJ, Park HL, Kim TW, Lee HS (2005) J Mat Sci 40:4089
7. Edelstein AS, Cammarata RC (1996) In: Nanomaterials: synthesis, properties and applications. Institute of Physics Publishing, Bristol and Philadelphia, p 145
8. Selomulya R, Ski S, Pita K, Kam CH, Zhang QY, Buddhudu S (2003) Mat Sci Eng B 100:136